The Journal of Immunology

# ISG15-Induced IL-10 Is a Novel Anti-Inflammatory Myeloid Axis Disrupted during Active Tuberculosis



Paula Fernandes dos Santos, Johan Van Weyenbergh, Murilo Delgobo, Daniel de Oliveira Patricio, Brian J. Ferguson, Rodrigo Guabiraba, Tim Dierckx, Soraya Maria Menezes, André Báfica and Daniel Santos Mansur

*J Immunol* 2018; 200:1434-1442; Prepublished online 8 January 2018;
doi: 10.4049/jimmunol.1701120
http://www.jimmunol.org/content/200/4/1434



*The Journal of Immunology* is published twice each month by
The American Association of Immunologists, Inc.,
1451 Rockville Pike, Suite 650, Rockville, MD 20852

Print ISSN: 0022-1767 Online ISSN: 1550-6606.

# ISG15-Induced IL-10 Is a Novel Anti-Inflammatory Myeloid Axis Disrupted during Active Tuberculosis

**Paula Fernandes dos Santos,* Johan Van Weyenbergh,† Murilo Delgobo,* Daniel de Oliveira Patricio,* Brian J. Ferguson,‡ Rodrigo Guabiraba,§ Tim Dierckx,† Soraya Maria Menezes,† André Báfica,* and Daniel Santos Mansur*,[1]**

**IFN-stimulated gene 15 (ISG15) deficiency in humans leads to severe IFNopathies and mycobacterial disease, the latter being previously attributed to its extracellular cytokine-like activity. In this study, we demonstrate a novel role for secreted ISG15 as an IL-10 inducer, unique to primary human monocytes. A balanced ISG15-induced monocyte/IL-10 versus lymphoid/IFN-γ expression, correlating with p38 MAPK and PI3K signaling, was found using targeted in vitro and ex vivo systems analysis of human transcriptomic datasets. The specificity and MAPK/PI3K-dependence of ISG15-induced monocyte IL-10 production was confirmed in vitro using CRISPR/Cas9 knockout and pharmacological inhibitors. Moreover, this ISG15/IL-10 axis was amplified in leprosy but disrupted in human active tuberculosis (TB) patients. Importantly, ISG15 strongly correlated with inflammation and disease severity during active TB, suggesting its potential use as a biomarker, awaiting clinical validation. In conclusion, this study identifies a novel anti-inflammatory ISG15/IL-10 myeloid axis that is disrupted in active TB.** ***The Journal of Immunology*****, 2018, 200: 1434–1442.**

Type I IFNs (IFN-I) exert most of their functions by inducing the expression of IFN-stimulated genes (ISGs). To date, over 300 ISGs have been described (1, 2) and ISG15, which is 15 KDa, is prominently expressed in response to infection, in autoimmune diseases, cancer, and physiological processes such as pregnancy (3–8). ISG15 is synthesized as a 17 KDa precursor that is cleaved in the C-terminal region, producing a mature form of 15 KDa. Also called ubiquitin cross-reactive protein, ISG15 was the first ubiquitin-like protein to be described and it can be covalently linked to other proteins in a process called ISGylation (3, 9–11). ISGylation is important for cell intrinsic immunity against several viruses including influenza A, vaccinia, Ebola, HIV, and hepatitis C virus (9, 12, 13).

In addition to its intracellular ISGylation-mediated processes, the mature form of ISG15 can be secreted and possesses cytokine-like activities that modulate leukocyte functions (3, 14). For instance, soluble ISG15 was found to enhance production of IFN-γ by lymphocytes and NK cells (15, 16), and to stimulate NK cell proliferation (16) as well as neutrophil migration (17). Importantly, ISG15 deficiency in humans is associated with a severe Mendelian susceptibility to mycobacterial disease (15) and cells from patients with a non-sense mutation or a frame-shift in *isg15* are deficient in IFN-γ–mediated immunity. This activity is attributed to the effects of extracellular ISG15 in NK cells and possibly occurs through an unknown receptor (15). Furthermore, humans lacking ISG15 also develop exacerbated IFN-I–induced immunopathology (18). This evidence suggests that extracellular or free ISG15, especially in humans (19), may regulate multiple aspects of the host immune response to pathogens and implicates this protein as an important component induced during infection and inflammatory processes involving IFN-I signaling. However, despite its ability to induce proinflammatory mediators, IFN-I may also exert anti-inflammatory effects (20–22), and whether soluble extracellular ISG15 modulates anti-inflammatory responses has not been reported.

This study demonstrates that ISG15 induces IL-10 synthesis in human primary monocytes through MAPK- and PI3K-dependent

*Laboratório de Imunobiologia, Departamento de Microbiologia, Imunologia e Parasitologia, Centro de Ciências Biológicas, Universidade Federal de Santa Catarina, Santa Catarina CEP 88040-900, Brazil; †Department of Microbiology and Immunology, Rega Institute for Medical Research, Laboratory for Clinical and Epidemiological Virology, KU Leuven - University of Leuven, 3000 Leuven, Belgium; ‡Department of Pathology, University of Cambridge, Cambridge CB2 1QP, United Kingdom; and §Infectiologie et Santé Publique, Institut National de la Recherche Agronomique, Université François Rabelais de Tours, 37380 Nouzilly, France

[1]D.S.M. is lead contact.

ORCIDs: 0000-0002-8881-672X (P.F.d.S.); 0000-0003-3234-8426 (J.V.W.); 0000-0003-4010-1909 (M.D.); 0000-0001-8318-3778 (D.d.O.P.); 0000-0002-6873-1032 (B.J.F.); 0000-0003-4005-1753 (R.G.); 0000-0002-1969-7974 (T.D.); 0000-0003-4519-8682 (S.M.M.); 0000-0002-5148-600X (A.B.); 0000-0001-6773-9334 (D.S.M.).

Received for publication August 10, 2017. Accepted for publication December 11, 2017.

This work was supported by Comissao de Aperfeiçoamento de Pessoal de Nível Superior (CAPES) Computational Biology (23038.010048/2013-27), Conselho Nacional de Desenvolvimento Científico e Tecnológico Universal (473897/2013-0), and the Academy of Medical Sciences/U.K. (NAF004/1005). P.F.d.S. and M.D. received CAPES and Conselho Nacional de Pesquisas (CNPq) student fellowships, respectively. A.B. received financial support from the National Institutes of Health Global Research Initiative Program (TW008276) and the Howard Hughes Medical Institute ECS (55007412). A.B. is a CNPq-PQ scholar and was supported by CAPES/ESE. B.J.F. received support from an Isaac Newton Trust/Wellcome Trust Institutional Strategic Support Fund/University of Cambridge research grant and a Wellcome Trust Seed Award (201946/Z/16/Z). T.D. received grant support from Agentschap Innoveren en Ondernemen (IWT141614). J.V.W. received grant support from CAPES (PVE) and the FWO (G0D6817N).

P.F.d.S., J.V.W., and R.G. designed and performed experiments, analyzed the data, and wrote the manuscript; M.D., D.d.O.P., T.D., and S.M.M. performed experiments and analyzed the data, B.J.F., A.B., and D.S.M. designed experiments, analyzed the data, and wrote the manuscript.

The microarray data presented in this article have been submitted to the Gene Expression Omnibus database (http://www.ncbi.nlm.nih.gov/geo/) under accession number GSE80008.

Address correspondence and reprint requests to Dr. Daniel Santos Mansur and Dr. André Báfica, Universidade Federal de Santa Catarina, Florianopolis, Santa Catarina CEP 88040-900, Brazil. E-mail addresses: daniel.mansur@ufsc.br (D.S.M.) and andre.bafica@ufsc.br (A.B.)

The online version of this article contains supplemental material.

Abbreviations used in this article: FSC, forward scatter; IFN-I, type I IFN; ISG, IFN-stimulated gene; KO, knockout; TB, tuberculosis; WT, wild type.



www.jimmunol.org/cgi/doi/10.4049/jimmunol.1701120

pathways. Additionally, analysis of human transcriptome datasets identified a myeloid *ISG15/IL-10* axis present in homeostasis. In contrast, the *ISG15/IL-10* axis is disrupted during active tuberculosis (TB) and *ISG15* mRNA levels strongly correlate with inflammatory and disease severity markers. These data suggest ISG15 may play a role in the cross-talk between IFNI/II and IL-10 and reveal *ISG15* mRNA levels as potentially useful biomarker in human active TB.

## Materials and Methods

### *Reagents*

ISG15 was purchased from Boston Biochem and tested for endotoxins by R&D Systems (endotoxin value for lot DBHF0614021 is <0.00394 EU/μg). *Limulus* amebocyte lysate assay (Lonza) was performed according to the manufacturer's instructions and the endotoxin level of recombinant ISG15 was below the detection threshold. Pro-ISG15 (UL-615) was also purchased from Boston Biochem. *Escherichia coli* LPS (strain O111:B4) (InvivoGen) was used as a positive control for IL-10 production in human PBMCs and monocytes. P38 kinase inhibitors SB203580 and SB220025 (Calbiochem) were used at 10 μM, MEK1/2 inhibitor U0126 (Cell Signaling) at 50 μM, and PI3K inhibitor Ly294002 (Cell Signaling) was at 50 μM. Solvent (DMSO, medium) was used as negative control and chloroquine (5 μg/ml; Sigma-Aldrich), a DNA-PKC/TLR endosomal signaling inhibitor, was used as an additional negative control.

### *Primary human cells*

Human PBMCs were separated from healthy individuals using Ficoll-Paque (GE) according to the manufacturer's instructions. Briefly, blood was collected in heparin-containing tubes, and gently mixed 1:1 with saline solution before being added over one volume of Ficoll-Paque reagent. The gradient was centrifuged for 35 min at 400 × *g*, 18°C. PBMCs were harvested and washed once with 45 ml of saline solution for 10 min at 400 × g, 18°C. Subsequently, the cell pellet was suspended and washed twice with 5 ml of saline solution for 10 min at 200 × g, 18°C to remove platelets. The remaining cell pellet was suspended to the desired density in RPMI 1640 (Life Technologies) supplemented with 5% FCS (Hyclone), 2 mM L-glutamine (Life Technologies), 1 mM sodium pyruvate (Life Technologies), 25 mM HEPES (Life Technologies), 100 U/ml penicillin, and 100 μg/ml streptomycin (Life Technologies). Cells were plated as described in each experiment. Human primary monocytes ($CD14^+$ cells) were separated from PBMCs using CD14 microbeads (Miltenyi Biotec) according to the manufacturer's instructions with the exception of the MACS buffer, which was prepared using 3% FCS. Monocyte enrichment varied between 73 and 92% between experiments. The use of PBMCs from healthy donors was previously approved by the Universidade de Santa Catarina ethical committee (Institutional Review Board 283/08).

### *Generation of isg15 knockout cell lines*

A549 lung epithelial cells were cotransfected with three gRNA/Cas9/GFP plasmids (provided by Horizon) targeting the *ISG15* locus using JetPEI (PolyPlus Transfection). The guide RNAs used were 5′-GGCTGTGGGCTGTGGGCTGT-3′, 5′-GGTAAGGCAGATGTCACAGG-3′ and 5′-TGGAGCTGCTCAGGGACACC-3′. Then 72 h after transfection, cells were sorted for GFP fluorescence then separated by limiting dilution. Single-cell derived clones were selected for ISG15 expression (Supplemental Fig. 1B).

### *A549: $CD14^+$ coculture*

A549 wild type (WT) or ISG15 knockout (KO) cells were seeded at $2 \times 10^5$ cells per ml in 24-well plates. Cells rested in the incubator for 6 h before ISG15 KO cells were transfected with ISG15-pCEP4 plasmid using FugeneHD reagent (Promega) according to the manufacturer's instructions. Cells were then washed and LPS was added 18 h after transfection and immediately prior to the addition of a $2 \times 10^5$ $CD14^+$ cell overlay. Following 24 h of coculture, supernatants were harvested for IL-10 quantification.

### *Immunoblotting*

Next, $1 \times 10^5$ $CD14^+$ cells were added to a 96-well plate and left to rest overnight. Cells were stimulated with ISG15 (1 μg/ml) and, after 15 min, spun at 4°C, supernatant was removed, and M-PER lysis buffer (Thermo Fisher Scientific) containing protease inhibitors (Complete, Mini Protease Inhibitor Tablets, Roche) and phosphatase inhibitors (#524625; Calbiochem) was added. Protein separation was performed according to the M-PER manufacturer's instructions. Abs concentrations for detection of p38 (9212; Cell Signaling) and p-p38 (9211; Cell Signaling), ISG15 (Cat: A600; R&D Systems), and anti–α-Tubulin (clone DM1A; Millipore) were those suggested by the manufacturers. For Western blots, at least 20 μg of total protein were separated and transferred to a polyvinylidene difluoride 0.22 μm blotting membrane. Membrane was blocked for at least 1 h with 1× TBST with 5% w/v nonfat dry milk and subsequently washed three times with TBST for 5 min each wash. Membrane was incubated with primary Abs diluted in 5% w/v BSA, 1× TBS, 0.1% Tween 20 at 4°C with gentle shaking overnight. Membrane was washed three times for 5 min each with TBST and then incubated with the appropriate secondary HRP-linked Ab for 1 h at room temperature. Membrane was washed three times, 5 min each with TBST before detection with ECL chemiluminescent substrate (Pierce).

### *p38 MAPK and PI3K signaling pathway inhibition*

Next, $1 \times 10^5$ $CD14^+$ cells were added to a 96-well plate and left to rest overnight. Inhibitors were added to cells for 1 h prior to ISG15 treatment. Then 24 h after treatment, cells were spun at 4°C, supernatant was harvested, and IL-10 was quantified by ELISA.

### *Cytokine quantification*

For exploratory experiments, IL-1β, IL-6, IL-10, IL-12p70, and TNF were quantified in supernatants by human inflammatory cytokine cytometric beads array kit (BD Biosciences). IL-10 and IFN-γ were quantified using a Human IL-10 DuoSet ELISA kit (R&D Systems) or Human IFN-γ mini kit (Thermo Fisher Scientific) according to the manufacturer's instructions.

### *Flow cytometry assays*

PBMCs were seeded at a density of $5 \times 10^5$ cells per well in 150 μl of medium. After 8 h of resting at 37°C with 5% $CO_2$, cells were treated with ISG15 (2 μg/ml) or LPS (1 μg/ml), unless indicated otherwise. Golgi Plug protein transport inhibitor (BD Biosciences) was added 1 h posttreatment, according to the manufacturer's instructions. Then, 12 h posttreatment, growth medium was removed and cold 1× HBSS (Life Technologies) with 2.5 mM EDTA was added to each well. The tissue culture dish was kept at 4°C for 30 min and cells were suspended and transferred to 1.5 ml tubes. Cells were washed in a final volume of 1 ml cold 1× HBSS (Life Technologies) with 2.5 mM EDTA at 300 × g and 4°C for 5 min. Supernatant was removed and cells were suspended in FACS buffer (1% BSA, 1% sodium azide in 1× PBS). Anti–human Ab mix containing anti-CD4 allophycocyanin-Cy7 (clone OKT1) (BioLegend), anti-CD8 PE-Cy7 (clone SK1) (BioLegend), anti-CD14 PerCP-Cy5.5 (clone M5E2) (BioLegend), and anti-CD56 FITC (clone NCAM 16.2) (BD Biosciences) was added to the cell suspension for 40 min at 4°C in the presence of 10% AB blood-type human serum to block Fc receptors. Afterwards, cells were washed once with 1 ml of 1× PBS at 300 × g, 4°C, for 5 min, and 1 ml of fixation buffer (1% paraformaldehyde in 1× PBS) was added to the cells. Tubes were kept in the dark at room temperature for 15 min and then centrifuged at 300 × *g*, 4°C, for 10 min to remove supernatant. Then, 1 ml of permeabilization buffer (0.5% saponin in FACS buffer) was added to the cells and tubes were centrifuged at 300 × *g*, 4°C for 10 min. Intracellular stain with anti–IL-10–PE (clone JES3-9D7) (BioLegend) was carried out for 30 min in the dark at room temperature. Cells were washed with permeabilization buffer at 300 × g, 4°C, 5 min, supernatant was removed, and cells were suspended in FACS buffer prior to acquisition of $1 \times 10^5$ events or more. For analysis, all acquired events displayed as forward scatter (FSC) and side scatter parameters were selected. After that, single-cell events were selected using FSC area and height parameters (FSC-A × FSC-H) and autofluorescence was excluded using allophycocyanin as an open channel. Intracellular IL-10 was then quantified in monocytes ($CD14^+IL\text{-}10^+$), NK cells ($CD56^+IL\text{-}10^+$), CD4 ($CD4^{high}IL\text{-}10^+$), and CD8 T cells ($CD8^{high}IL\text{-}10^+$). Gates were set according to unstained PBMC sample and controls. All samples were acquired on a Becton-Dickinson Verse flow cytometer using BD FACSuite software. To analyze cell death, $5 \times 10^5$ PBMC per well were treated with ISG15 2 μg/ml or staurosporine (Sigma-Aldrich) 1 μM for 24 h. Cells were then harvested, washed with 1 ml of PBS at 300 × g, room temperature, 5 min, then supernatant was removed and cells were washed once in 1 ml of 1× annexin binding buffer (eBioscience). Cells were resuspended at $10^6$ cells per ml in 1× annexin binding buffer and FITC conjugated annexin V (eBioscience) was added to the cell suspension for 15 min, room temperature, according to the manufacturer's instruction. Following incubation period, cells were washed with 1 ml of 1× annexin binding buffer, 300 × g, room temperature, 5 min, and resuspended in 200 μl of 1× annexin binding buffer. Propidium iodide (BD Pharmingen) was added at 0.25 μg/ml to the cell suspension

prior to sample acquisition. Samples were acquired on a Becton-Dickinson Canto II flow cytometer using BD FACSDiva software.

### *Real-time quantitative PCR*

For relative quantification of *IL-10* gene expression, total RNA was extracted from PBMCs treated or not with ISG15. RNA was extracted after 6, 12, 24, or 48 h of treatment using an RNeasy RNA extraction kit (Qiagen). Using 400 ng of RNA, cDNA was produced with a High-Capacity cDNA Reverse Transcription Kit (Applied Biosystems) and 2 μl of the product was used for the quantitative PCR reaction in a final volume of 10 μl. Quantitative PCR reactions were performed using the primers forward 5′-GAG ATC TCC GAG ATG CCT TCA G-3′and reverse 5′-CAA GGA CTC CTT TAA CAA CAA GTT GT-3′ (23). Fold-increase in *IL-10* gene expression was determined by relative quantification using hypoxanthine phosphoribosyltransferase (*HPRT*) as endogenous control. Primers forward and reverse for *HPRT* were 5′-CCTGCTGGATTACATCAAAGCACTG-3′ and 5′-TCCAACACTTCGTGGGGTCCT-3′, respectively, and were used at 250 nM each.

### *Microarray analysis*

Curated and annotated publicly available datasets (24–29) (GXB, ImmuCo, ImmuSort, BioGPS, GEO) were obtained from large, established cohorts of healthy controls, latent, and active TB patients, comprising ex vivo and in vitro whole blood, total PBMCs, purified leukocyte subsets, nonleukocyte human primary cells, and skin biopsies (leprosy patients, healthy controls, and cutaneous leishmaniasis as nonmycobacterial infectious control). Novel datasets were generated for both whole blood and PBMCs from healthy controls and individuals infected with another nonmycobacterial intracellular pathogen (*Leishmania braziliensis*). Data from the healthy controls were used in this study. PBMCs were isolated as above and immediately frozen in Trizol to preserve RNA integrity. Following Trizol extraction, total RNA was further purified using an RNeasy kit according to the manufacturer's protocol (Qiagen, Venlo, the Netherlands). Affymetrix Whole Genome microarray analysis was performed by the VIB Nucleomics Facility (Leuven, Belgium) using a GeneChip Human Gene 1.0 ST Array with the WT PLUS reagent kit (Affymetrix, Santa Clara, CA) according to the manufacturer's specifications. Data preprocessing (RMA) was performed using the Bioconductor xps package. All microarray raw data are available at Gene Expression Omnibus database (http://www.ncbi.nlm.nih.gov/geo/) under series accession number GSE80008.

### *Enrichment analysis*

The Ingenuity Pathway Analysis program was used to perform the initial pathway and function level analysis on genes determined to be differentially expressed in the microarray analysis (Ingenuity Systems, Red Wood City, CA). Uncorrected $p$ values and absolute fold-changes were used with cutoffs of $p < 0.05$. Based on a scientific literature database, the genes were sorted into gene networks and canonical pathways, and significantly overrepresented pathways were identified. Further enrichment analysis was performed, including Gene Ontology term enrichment using the WEB-based GEne SeT AnaLysis Toolkit (WebGestalt), KEGG pathway enrichment using the pathway database from the Kyoto Encyclopedia of Genes and Genomes, and transcription factor target enrichment using data from the Broad Institute Molecular Signatures Database (MSigDB). Genesets from the Gene Ontology, KEGG pathways, WikiPathways, and Pathway Commons databases, as well as transcription factors, were considered overrepresented if their corrected $p$ value was smaller than 0.05. Principal component analysis, correlation matrices (Spearman), and unsupervised hierarchical (Euclidian distance) clustering were performed using XLSTAT, and visualized using MORPHEUS (https://software.broadinstitute.org/morpheus/).

### *Data processing and statistical analyses*

Data derived from in vitro experiments was processed using GraphPad Prism 6 and analyzed using an unpaired Student $t$ test unless stated otherwise. Statistical significance is expressed as follows: $*p < 0.05$, $**p < 0.01$, $***p < 0.001$, $****p < 0.0001$. In all cases, data shown are representative from at least two independent experiments. Data from experiments performed in triplicate are expressed as mean ± SEM.

## Results

### *ISG15 induces IL-10 production in human PBMCs*

Extracellular ISG15 stimulates IFN-γ production by human NK cells (15), so to investigate whether ISG15 regulates synthesis of other inflammatory cytokines, PBMCs were exposed to soluble ISG15 and 24 h cell culture supernatants assayed for several cytokines by cytometric bead array. Of this panel, only IL-10 and IL-6 were induced by ISG15 (Supplemental Fig. 1A). IL-10 is a key immune-regulatory cytokine that exerts opposing effects to IFN-γ, hence this result was further assessed by treating PBMCs with different concentrations of pro- or mature ISG15 indicating a concentration-dependent response (Fig. 1A). Following intracellular processing of pro-ISG15, its C-terminal LRLRGG domain is exposed and the protein becomes mature, a necessary requirement for ISGylation (11, 30–32). Both pro- and mature ISG15 induced IL-10 secretion in human PBMCs in a similar manner (Fig. 1A), indicating that LRLRGG sequence does not need to be exposed for ISG15-mediated IL-10 production. Exogenous ISG15 stimulated IL-10 synthesis by PBMCs from most of the healthy donors tested (Fig. 1B). Control experiments showed that heat-denatured ISG15 did not promote IL-10 synthesis, demonstrating this protein requires its correctly folded structure to induce cell signaling (Fig. 1B). Kinetic analysis of ISG15 stimulation in human PBMCs showed a peak of IL-10 mRNA and protein synthesis after 6 and 12 h respectively (Fig. 1C, 1D). In contrast, other ISGs such as IFN-α and CCL5 did not induce IL-10 production by human PBMCs (Supplemental Fig. 1C–F). Interestingly, this response was found to be specific for primary cells as a library of human cell lines (NKL, NK92, THP-1, Karpas, U937, and Jurkat) treated with ISG15 did not produce IL-10 (data not shown). Additionally, ISG15 treatment did not induce cell death by means of annexin V expression and propidium iodide incorporation (Fig. 1E–G), suggesting IL-10 was actively secreted, not released from nor induced by apoptotic or necrotic cells. Together, these data show that ISG15 induces IL-10 synthesis and secretion by primary human PBMCs, independent of cell death.

### *$CD14^+$ cells are the main producers of ISG15-induced IL-10*

ISG15 can act on different cell types (15–17, 33), hence intracellular cytokine staining was used to identify the source of ISG15-induced IL-10 in PBMC subpopulations. These experiments indicated that $CD14^+$ cells are the main source of IL-10 (Fig. 2A) with an average 2.5-fold increase of $CD14^+IL\text{-}10^+$ cells as compared with unstimulated cultures (Fig. 2B). Next, PBMCs were separated into $CD14^+$ and $CD14^-$ populations and both groups were exposed to soluble ISG15. Quantification of IL-10 and IFN-γ 24 h poststimulation confirmed the $CD14^+$ population to be the main producers of IL-10 (Fig. 2C) and we corroborated previous work showing the $CD14^-$ population to be the source of ISG15-induced IFN-γ (Fig. 2D) (15, 16). Additionally, these data indicate that recombinant ISG15-induced IL-10 synthesis by $CD14^+$ populations does not require the presence of $CD14^-$ cells.

To test whether endogenously produced ISG15 stimulates IL-10 synthesis, a coculture experiment was set up using a lung epithelial cell line, A549, as a source of ISG15 (34). For these assays, an *ISG15*-KO A549 cell line was generated using CRISPR/Cas9 technology (Supplemental Fig. 1B, clone 3). WT or *ISG15*-KO A549 cells were then cocultured with purified human primary $CD14^+$ cells or stimulated with LPS as a positive control. In this setup, A549-monocyte cocultures led to a consistent production of IL-10, an outcome completely abrogated when *ISG15*-KO A549 cells were used. This effect could be rescued by reintroduction of the *ISG15* gene into the KO cells (Fig. 2E), thus demonstrating the specificity of epithelial cell–derived ISG15 for the induction IL-10.

To study coregulation of *ISG15*/*IL-10*/*IFNG* pathways in different cell types ex vivo, we next examined transcriptome datasets of purified major human leukocyte subsets (ImmuCo, ImmuSort) (28, 29). Expression levels of *ISG15* and *IL-10* are positively correlated in total PBMCs, purified monocytes, and macrophages, but not neutrophils and T cells (Fig. 2F–J). Although neutrophils display the highest *ISG15*/*IL-10* expression ratio, monocytes are the

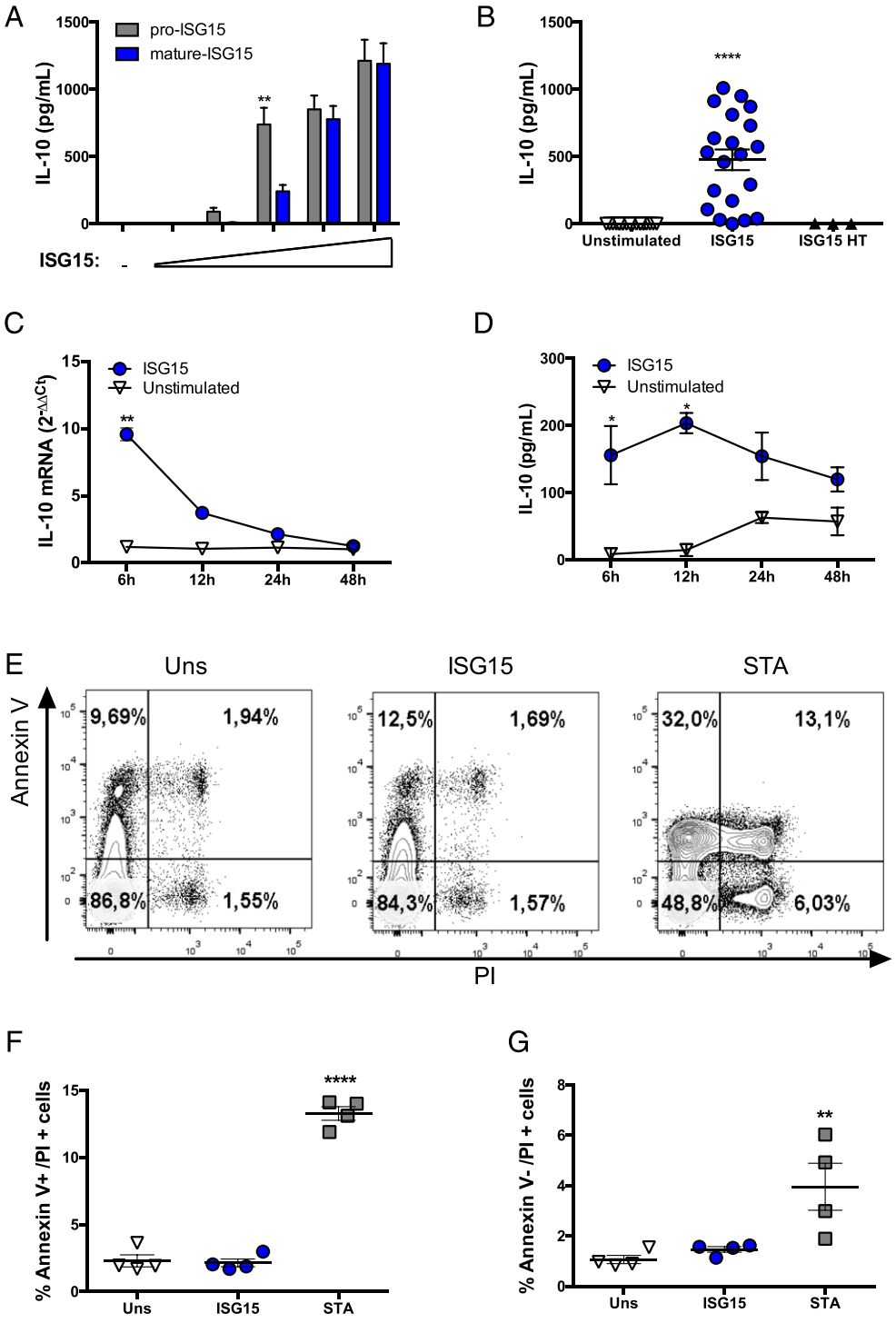


**FIGURE 1.** ISG15 induces the production of IL-10 in human PBMCs. (**A**) Dose-dependent IL-10 production was measured by ELISA 24 h poststimulation of PBMCs with both pro- and mature ISG15 [(ISG15): 0.15; 0.45; 1.5, 4.5, and 15 μg/ml]. (**B**) Induction of IL-10 by recombinant, but not heat-treated, ISG15 using PBMCs from a total of five different donors in eight independent experiments. (**C**) *IL-10* mRNA expression in PBMCs treated with ISG15 at 6, 12, 24, and 48 h poststimulation. (**D**) Quantification of IL-10 in the supernatant of human PBMCs at 6, 12, 24, and 48 h after treatment with of ISG15. (**E**) Representative dot plot evaluating cell-death in human PBMCs by annexin V and PI staining after treatment with ISG15 (2 μg/m) or staurosporine (1 μM). (**F** and **G**) Quantification of cell death from the experiment described in (E). Unless stated otherwise, ISG15 concentration was 1.5 μg/ml. Error bars indicate SEM for biological replicates in each experiment. In each experiment PBMCs from three or more different donors were used. $*p < 0.05$, $**p < 0.01$, $****p < 0.0001$. ISG15HT, ISG15 heat-treated; STA, staurosporine; PI, propidium iodide; Uns, unstimulated.

main ex vivo *IL-10*–expressing cell type (60.19% of cells with *IL-10* transcripts above detection limit, versus 17.33% in PBMCs and 5.97% in neutrophils, Fig. 2K), thus corroborating our in vitro results (Fig. 2A–D). Consistent with a previous study (35), low or undetectable *IL-10* transcripts in human neutrophils (Fig. 2K) are explained by the inactive chromatin configuration of the *IL-10* locus in these cells. Together, this set of results suggests a role for extracellular rather than intracellular ISG15 as a paracrine inducer of monocyte-derived IL-10 (shown by this study) and NK-derived IFN-γ (15). Because the unique susceptibility of ISG15-deficient

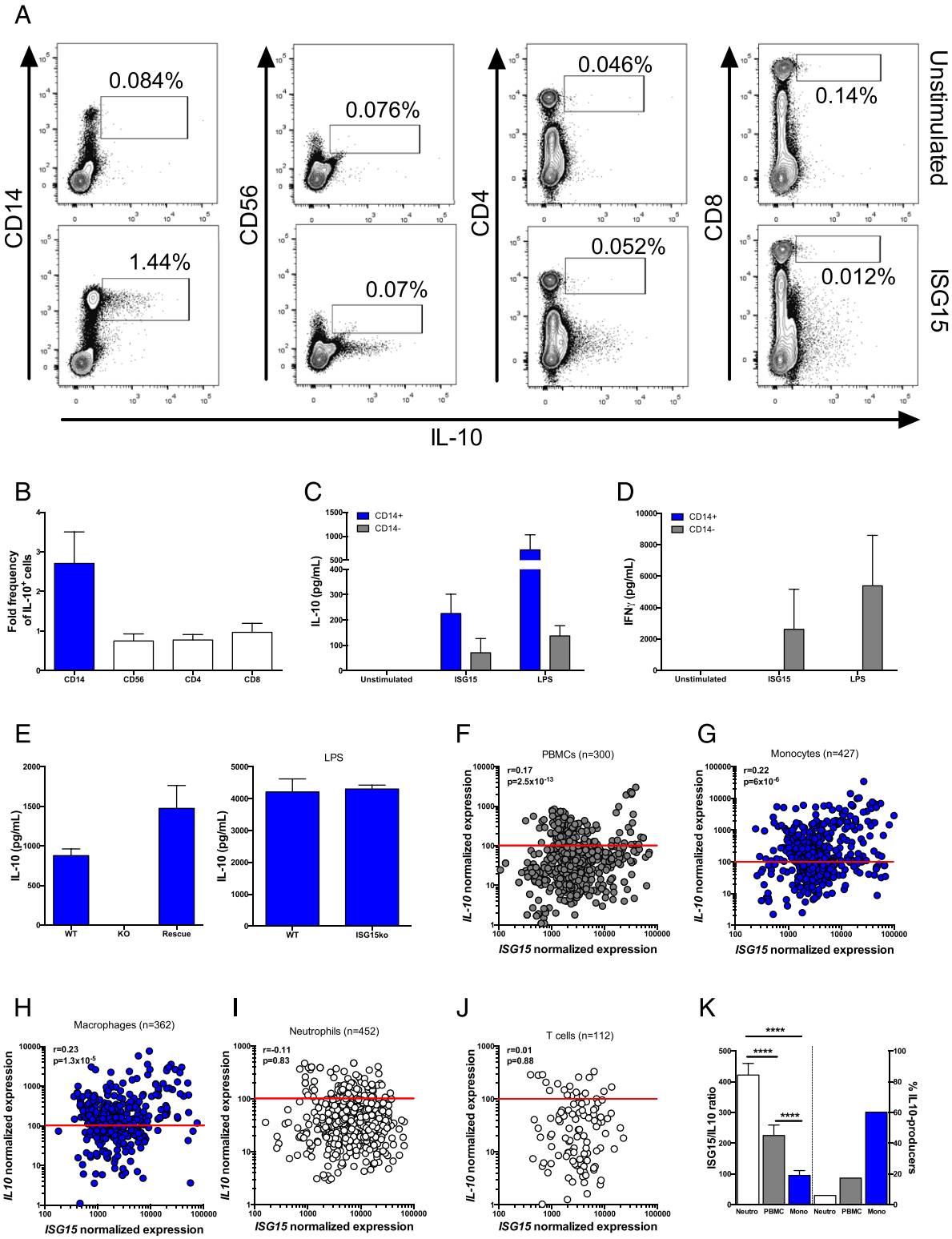


**FIGURE 2.** CD14$^+$ cells are the main source of IL-10 upon ISG15 stimulation. (**A**) Representative dot plot of intracellular staining of IL-10 in CD14$^+$, CD56$^+$, CD4$^+$, and CD8$^+$ in ISG15-treated PBMCs. (**B**) PBMCs from six different individuals showing fold increase in IL-10 production from CD14$^+$, CD56$^+$, CD4$^+$, and CD8$^+$ populations after ISG15 stimulation. (**C** and **D**) ELISA quantification of IL-10 and IFN-γ in the supernatants of CD14$^+$ and CD14$^-$ separated populations treated with ISG15 (**E**) A549 WT or ISG15 KO cells were cocultured with primary CD14$^+$ cells magnetically separated from PBMCs and IL-10 production was measured by ELISA 24 h later. *ISG15* KO cells were also transfected with a plasmid expressing *ISG15* to rescue its function. LPS was used as a positive control for IL-10 stimulation. Error bars indicate SEM for biological replicates in each experiment. All experiments were repeated at least two times. In every experiment PBMCs from three or more donors were used. (**F**–**J**) Transcriptome datasets of healthy controls (ImmuCo, ImmuSort) confirm *ISG15* and *IL-10* ex vivo expression levels are positively correlated in total PBMCs (F), purified primary monocytes (G), and macrophages (H), but not neutrophils (I) or T cells (J). Red lines indicate the approximate threshold for *IL-10* mRNA detection (determined for each individual microarray). (**K**) Neutrophils display the largest *ISG15*/*IL-10* ratio ex vivo, whereas monocytes are the major *IL-10*-expressing leukocyte population (> PBMCs > neutrophils) under homeostatic conditions. ****$p < 0.0001$.

children to low-virulence mycobacteria has underscored a role for extracellular ISG15 (15), we performed a systems analysis approach to gain insight in the possible influence of ISG15/IL-10 axis during mycobacterial exposure in humans.

### *IL-10 production in response to ISG15 requires MAPK-PI3K signaling pathways*

MAPK and PI3K signaling pathways have been shown to participate in *IL-10* transcription in human monocytes and macrophages. For instance, p38, ERK1/2, and PI3K are crucial for IL-10 synthesis during microbial stimuli such as LPS and *Mycobacterium* (36, 37). Thus, we analyzed a published transcriptome dataset of latent TB using WebGEstalt and Ingenuity Pathway Analysis. MAPK and PI3K signaling pathways were significantly enriched in latent TB transcriptomes, as compared with healthy uninfected controls (Supplemental Table I). We next investigated whether *ISG15*, *IL-10*, *IFNG*, and members of the MAPK and PI3K signaling families displayed divergent expression patterns between latent and active TB. In keeping with our hypothesis, an anti-inflammatory IL-10 monocyte axis (ISG15/IL-10/CD14 and downstream STAT3) was significantly unregulated, and a protective IFNG axis (CD8/NK and upstream STAT4) was significantly downregulated in active TB, whereas the opposite effect was observed in latent TB (Fig. 3A). Likewise, *MAPK3* and *PIK3CA* (PI3Kalpha) levels were unregulated in active TB and downregulated in latent TB. Interestingly, MAPK14 was unregulated in both latent and active TB (Fig. 3A). In this scenario, *MAPK14* (p38) expression levels were significantly and positively correlated to *ISG15* levels ex vivo (Fig. 3B). Additionally, *MAPK3* (MAP3K/ERK1) levels were positively correlated to *IL-10* (Fig. 3C) and negatively correlated to *IFNG* transcript levels (Fig. 3D). Finally, *PIK3CA* and *PIK3CB* (PI3Kbeta) transcripts were negatively correlated to *IL-10* expression levels (Fig. 3E). These data suggested that ISG15/IL-10 as well as MAPK/PI3K-associated transcripts are coregulated during mycobacterial stimulation in vivo and raised the possibility that MAPK/PI3K pathway is involved in ISG15-induced IL-10 responses in monocytes. Indeed, following exposure of $CD14^+$ cells to ISG15, increased phosphorylation of p38 MAPK was observed (Fig. 3F). More importantly, the use of two distinct inhibitors for p38 (Fig. 3G, 3H) as well as inhibitors for MEK1/2 (Fig. 3I) and PI3K (Fig. 3J) abrogated IL-10 production in ISG15-stimulated monocytes. In contrast, chloroquine, an inhibitor targeting DNA-PKCs/TLR9/endosome signaling pathways, did not affect IL-10 synthesis induced by ISG15 (Fig. 3J). These results suggest a central role for p38 activation and MAPK as well as PI3K signaling in ISG15-induced IL-10 production by primary monocytes.

### *An ISG15/IL-10/IFNG cluster in healthy controls is disrupted during active TB*

Altogether, our data indicated that ISG15 is associated with immunoregulatory responses and could have an important role in mycobacterial-induced inflammation. To test this concept, publicly available transcriptome datasets from established cohorts of healthy controls and patients with leprosy as well as latent or active TB were examined. Positive and negative correlations (Spearman Rho) were calculated between normalized transcript levels of MAPK/PI3K/STAT signaling family members, established myeloid lineage markers (*CD14*, CD16 = *FCGR3A/FCGR3B*, *ITGAM*, *ITGAX*), and lymphoid lineage markers (*CD4*, *CD8*, CD56 = *NCAM1*, *ITGAL*) plus *ISG15*, *IL-10* and *IFNG* transcripts. Unsupervised hierarchical clustering of these transcripts was then performed, based on the resulting correlation matrices. In healthy controls (Fig. 4A), *ISG15*

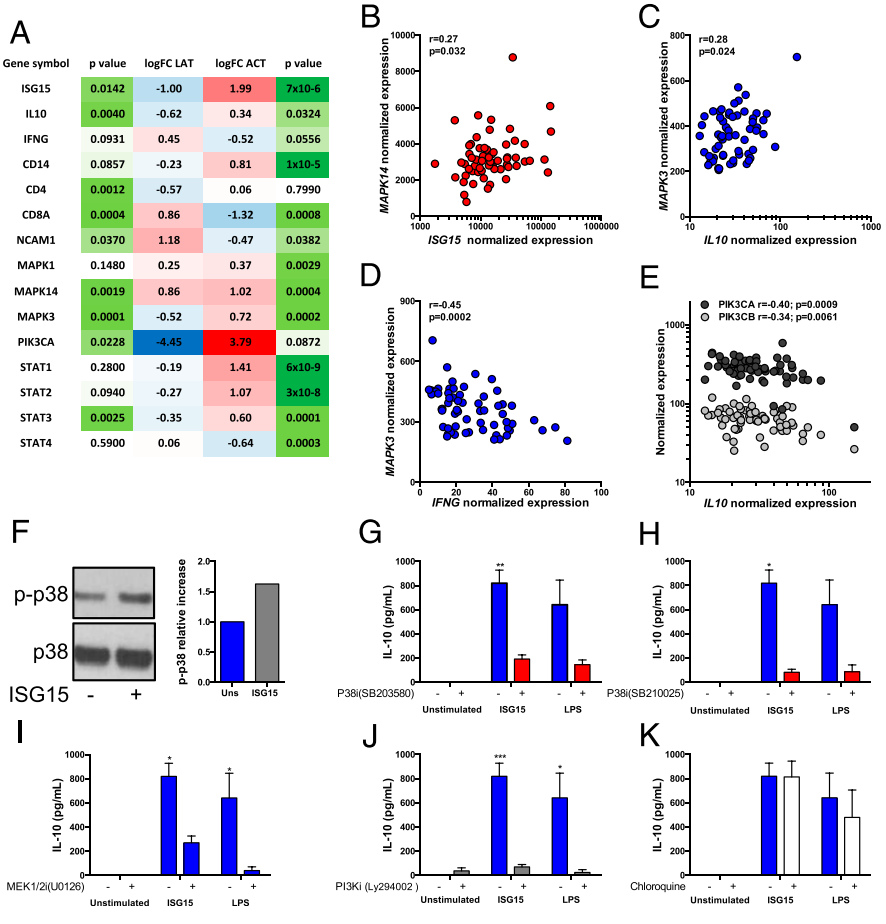


**FIGURE 3.** ISG15 induces monocyte-derived IL-10 via p38, MEK1/2, and PI3K signaling pathways, which are deregulated in human mycobacterial infections. (**A**) Differential gene expression of ISG15/IL-10/IFNG and their upstream and downstream (MAPK, PIK3, and STAT family members) signaling molecules, as well as cell type markers in latent versus active TB as compared with healthy controls [heatmap of fold-change (FC, blue = down, red = up) and *p* values (green, false discovery rate–corrected)]. Ex vivo expression level correlation of *MAPK14* and *ISG15* (**B**), *MAPK3* and *IL-10* (**C**), *MAPK3* and *IFNG* (**D**), and of *PIK3CA* or *PIK3CB* with *IL-10* (**E**) during latent TB infection (**F**) Representative immunoblot showing the phosphorylation of p38 MAPK 15 min after the stimulation of ISG15 in $CD14^+$ cells. (**G**–**J**) $CD14^+$ cells were treated for 1 h with p38 (10 μM), MEK1/2 (50 μM), and PI3K inhibitors (50 μM) (B–E respectively) prior to addition of ISG15 (1 μg/ml) or LPS (100 ng/ml). (**K**) Chloroquine (5 μg/ml) was used as an unrelated control drug. Then 24 h after treatment, supernatant was harvested and used for IL-10 quantification by ELISA. Error bars indicate SEM for three biological replicates in two independent experiments. $*p < 0.05$, $**p < 0.01$, $***p < 0.001$. Uns, unstimulated.

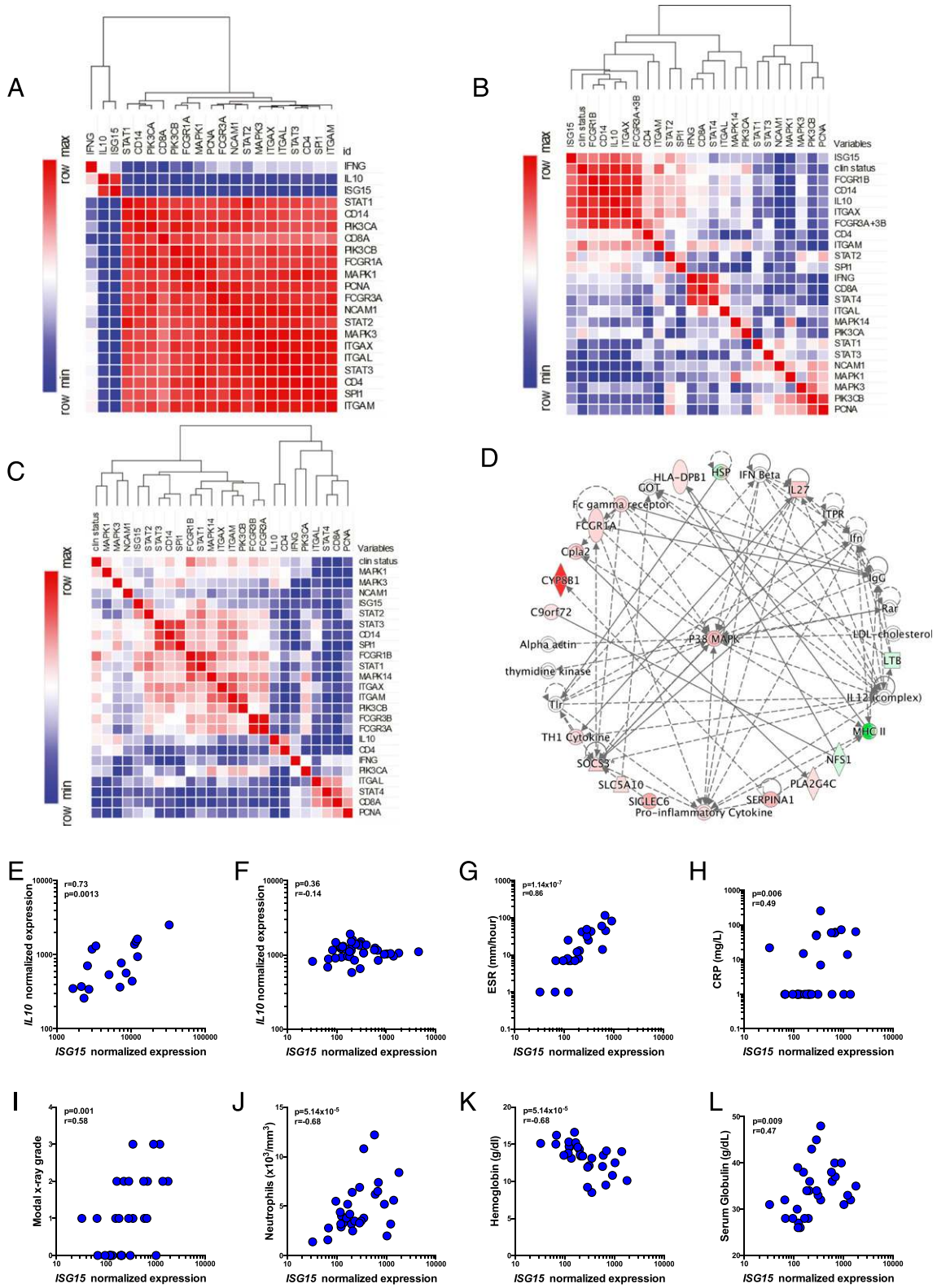


**FIGURE 4.** An anti-inflammatory *ISG15*/*IL-10* myeloid axis is amplified in human leprosy and disrupted in human TB, revealing a novel clinical biomarker. (**A**–**C**) Heatmaps representing positive (red) and negative (blue) correlation matrix of selected genes (see text) classified by unsupervised hierarchical clustering (Euclidian distance). (A) Healthy controls (GSE80008), (B) leprosy patients (GSE17763), (C) TB cohort (GSE28623). (**D**) Significantly enriched network (Ingenuity Pathway Analysis) showing p38 MAPK as highly interconnected in the monocyte transcriptome of TB patients. (**E** and **F**) *ISG15* transcript correlates with IL-10 transcript level in leprosy patients, but not in patients with active TB. (**G** and **H**) *ISG15* transcript level correlates with established inflammatory metrics [erythrocyte sedimentation rate (ESR), C-reactive protein (CRP)], (**I**) tissue damage (Modal X-ray grade), as well as (**J**–**L**) systemic clinical parameters (neutrophil count, hemoglobin, and globulin serum concentration) in patients with active TB.

mRNA strongly clusters with *IL-10*, and to a lesser extent with *IFNG*, indicating the existence of a regulatory balance between pro- and anti-inflammatory effects under homeostatic conditions. Leprosy lesions have been shown to express both IFN-I and IL-10, a scenario that leads to suppression of IFN-γ effector activities (27). An unsupervised hierarchical cluster analysis of the cohort published by Teles et al. shows the myeloid anti-inflammatory *ISG15*/*IL-10* axis was maintained in leprosy lesions (Fig. 4B), demonstrated by a single expression cluster comprised of *ISG15*, *IL-10* and monocyte (*CD14*) and myeloid markers (CD64 = *FCGR1*, CD11c = *ITGAX*, PU.1 = *SPI1*, CD16 = *FCGR3*). Consistent with previous data (27), this disease cluster was negatively correlated to a protective *CD8*/*IFNG*/*STAT4* cluster, which is associated with milder (borderline tuberculoid/paucibacillary) clinical form, whereas the *ISG15*/*IL-10*/*CD14* cluster was associated with the severe (lepromatous/multibacillary) disease form. Surprisingly, the *ISG15*/*IL-10* axis was disrupted in whole blood transcriptomes of active TB (Fig. 4C). However, ISG15 (but not *IL-10* or *IFNG*) retained its association with disease status and monocyte/myeloid markers (*CD14*, *FCGR1*). Because TB disease signature in the whole blood is predominated by neutrophils (24) and monocytes only make up a minor fraction in these samples, we next investigated whether components of the *ISG15*/*IL-10* signaling pathway might be overexpressed in purified monocytes from TB patients, as compared with control monocytes. Indeed, Ingenuity Pathway Analysis identified MAPK signaling as significantly enriched in monocytes from TB patients (data not shown), and p38 MAPK was significantly interconnected with several TB signature genes (*FCGR1*, *IL-27*, *SIGLEC6*) in a disease network (Fig. 4D). Together, these results show the *ISG15*/*IL-10* axis is disrupted during active TB.

To further investigate the possible connection between ISG15 and *M. tuberculosis*-mediated immunopathology, we examined the expression of this gene in an independent large cohort in which both detailed clinical parameters and corresponding transcriptome data are available (24). Expression levels of *ISG15* were significantly correlated with established inflammatory biomarkers such as erythrocyte sedimentation rate, C-reactive protein, tissue damage (Modal X-ray grade) as well as systemic clinical parameters (neutrophil count, hemoglobin, and globulin serum concentration) (Fig. 4G–L). These results suggest ISG15 may be a biomarker of disease severity in active TB patients.

## Discussion

Unconjugated ISG15 was shown previously to induce a variety of responses in different cells and contexts (3). Humans lacking ISG15 present severe mycobacterial disease and IFNopathy (15, 18), and it is interesting to notice that both phenotypes are possibly linked to this form of the protein and not due to ISGylation (19). Studies performed in mice lacking ISG15 or UbE1L, E1 enzyme necessary for most ISGylation processes (38), show a mild phenotype after *M. tuberculosis* infection (39), pointing to a contrasting role of ISG15 in mice and humans. This is reinforced by the fact that ISG15 deficiency in humans is not linked to a higher susceptibility to viral infections, as seen in mice (18, 40–43).

Exploring its extracellular role, we show that ISG15 induces IL-10 production in monocytes via a MAPK- and PI3K-dependent pathway. Activation of both of these pathways has been shown previously to be involved in *IL-10* transcription (44). Interestingly, it has been shown that IFN-γ production by NK cells, the main IFN-γ producers upon stimulation with ISG15, can also be mediated by MAPK and PI3K (45). This suggests that the ISG15 receptor, if common to both monocytes and NK cells, might use these common downstream signal transducers to exert its activities. This merits further investigation.

Although ISG15 is critical for IFN-γ production by cells from vaccine strain bacillus Calmette-Guérin–infected patients (15), this protein has a synergistic effect when combined with IL-12 (15), an important inducer of IFN-γ (46, 47). Furthermore, IL-10 inhibits production of IL-12 and, consequently, of IFN-γ by PBMCs (48), pointing to a pleiotropic effect for ISG15. Cell type- and context-dependent effects of ISG15 could explain these diverse activities. This work and others (15) suggest that, despite ubiquitous expression in different cell types, neutrophils are a major source of secreted ISG15. Additionally, *M. tuberculosis*–infected macrophages can release microparticles containing ISG15 in vitro (49). Although we have not tested this directly, we speculate that soluble phagocyte-derived ISG15 is important to the orchestration of immune responses in vivo, driving the production of at least two major cytokines, IL-10 and IFN-γ. Interestingly, the intra- and extracellular location of ISG15 and its ability to induce a plethora of effects in distinct cells resembles the function of an alarmin (50). As shown in Fig. 4, ISG15's function is context dependent, varying from a driver of an anti-inflammatory monocytic/IL-10 axis (present in homeostasis and amplified in *M. leprae* infection) to a strong proinflammatory IFN-γ–biased scenario during active TB. Additionally, because ISG15 and IL-10 lack correlation in active *M. tuberculosis* infection, it is possible that IL-10 is controlled by signals other than ISG15 during disease. Whether virulent *M. tuberculosis* hijacks the ISG15/IL-10 axis contributing to induction of tissue pathology remains to be determined.

In conclusion, these findings confirm and extend previous work characterizing soluble extracellular ISG15 as a pleiotropic cytokine (or alarmin) that induces both pro- and anti-inflammatory effects in a variety of cell types. Moreover, the combined ex vivo and in vitro approach uncovers a novel myeloid *ISG15*/*IL-10* p38-mediated anti-inflammatory signaling cascade, which is preserved in human leprosy but disrupted in active TB. Strikingly, our data indicate *ISG15* mRNA as a novel potential biomarker of disease severity during active TB that merits further investigation

## Acknowledgments

We thank Prof. Aristobolo Mendes Silva from Universidade Federal de Minas Gerais for providing reagents and suggestions, and Dr. Alan Sher for critical reading and evaluation of these results.

## Disclosures

The authors have no financial conflicts of interest.

## References

1. de Veer, M. J., M. Holko, M. Frevel, E. Walker, S. Der, J. M. Paranjape, R. H. Silverman, and B. R. Williams. 2001. Functional classification of interferon-stimulated genes identified using microarrays. *J. Leukoc. Biol.* 69: 912–920.
2. Der, S. D., A. Zhou, B. R. Williams, and R. H. Silverman. 1998. Identification of genes differentially regulated by interferon alpha, beta, or gamma using oligonucleotide arrays. *Proc. Natl. Acad. Sci. USA* 95: 15623–15628.
3. Dos Santos, P. F., and D. S. Mansur. 2017. Beyond ISGlylation: functions of free intracellular and extracellular ISG15. *J. Interferon Cytokine Res.* 37: 246–253.
4. Hansen, T. R., and J. K. Pru. 2014. ISGylation: a conserved pathway in mammalian pregnancy. *Adv. Exp. Med. Biol.* 759: 13–31.
5. Henkes, L. E., J. K. Pru, R. L. Ashley, R. V. Anthony, D. N. Veeramachaneni, K. C. Gates, and T. R. Hansen. 2015. Embryo mortality in Isg15$^{-/-}$ mice is exacerbated by environmental stress. *Biol. Reprod.* 92: 36.
6. Hermann, M., and D. Bogunovic. 2017. ISG15: in sickness and in health. *Trends Immunol.* 38: 79–93.
7. Tecalco Cruz, A. C., and K. Mejía-Barreto. 2017. Cell type-dependent regulation of free ISG15 levels and ISGylation. *J. Cell Commun. Signal.* 11: 127–135.
8. Wang, B. X., S. A. Grover, P. Kannu, G. Yoon, R. M. Laxer, E. A. Yeh, and E. N. Fish. 2017. Interferon-stimulated gene expression as a preferred biomarker

for disease activity in aicardi-goutieres syndrome. *J. Interferon Cytokine Res.* 37: 147–152.
9. Skaug, B., and Z. J. Chen. 2010. Emerging role of ISG15 in antiviral immunity. *Cell* 143: 187–190.
10. Haas, A. L., P. Ahrens, P. M. Bright, and H. Ankel. 1987. Interferon induces a 15-kilodalton protein exhibiting marked homology to ubiquitin. *J. Biol. Chem.* 262: 11315–11323.
11. Loeb, K. R., and A. L. Haas. 1992. The interferon-inducible 15-kDa ubiquitin homolog conjugates to intracellular proteins. *J. Biol. Chem.* 267: 7806–7813.
12. Morales, D. J., and D. J. Lenschow. 2013. The antiviral activities of ISG15. *J. Mol. Biol.* 425: 4995–5008.
13. Schoggins, J. W., and C. M. Rice. 2011. Interferon-stimulated genes and their antiviral effector functions. *Curr. Opin. Virol.* 1: 519–525.
14. Bogunovic, D., S. Boisson-Dupuis, and J. L. Casanova. 2013. ISG15: leading a double life as a secreted molecule. *Exp. Mol. Med.* 45: e18.
15. Bogunovic, D., M. Byun, L. A. Durfee, A. Abhyankar, O. Sanal, D. Mansouri, S. Salem, I. Radovanovic, A. V. Grant, P. Adimi, et al. 2012. Mycobacterial disease and impaired IFN-γ immunity in humans with inherited ISG15 deficiency. *Science* 337: 1684–1688.
16. D'Cunha, J., E. Knight, Jr., A. L. Haas, R. L. Truitt, and E. C. Borden. 1996. Immunoregulatory properties of ISG15, an interferon-induced cytokine. *Proc. Natl. Acad. Sci. USA* 93: 211–215.
17. Owhashi, M., Y. Taoka, K. Ishii, S. Nakazawa, H. Uemura, and H. Kambara. 2003. Identification of a ubiquitin family protein as a novel neutrophil chemotactic factor. *Biochem. Biophys. Res. Commun.* 309: 533–539.
18. Zhang, X., D. Bogunovic, B. Payelle-Brogard, V. Francois-Newton, S. D. Speer, C. Yuan, S. Volpi, Z. Li, O. Sanal, D. Mansouri, et al. 2015. Human intracellular ISG15 prevents interferon-α/β over-amplification and auto-inflammation. *Nature* 517: 89–93.
19. Speer, S. D., Z. Li, S. Buta, B. Payelle-Brogard, L. Qian, F. Vigant, E. Rubino, T. J. Gardner, T. Wedeking, M. Hermann, et al. 2016. ISG15 deficiency and increased viral resistance in humans but not mice. *Nat. Commun.* 7: 11496.
20. Billiau, A. 2006. Anti-inflammatory properties of Type I interferons. *Antiviral Res.* 71: 108–116.
21. Borden, E. C., G. C. Sen, G. Uze, R. H. Silverman, R. M. Ransohoff, G. R. Foster, and G. R. Stark. 2007. Interferons at age 50: past, current and future impact on biomedicine. *Nat. Rev. Drug Discov.* 6: 975–990.
22. McNab, F., K. Mayer-Barber, A. Sher, A. Wack, and A. O'Garra. 2015. Type I interferons in infectious disease. *Nat. Rev. Immunol.* 15: 87–103.
23. Skrzeczyńska-Moncznik, J., M. Bzowska, S. Loseke, E. Grage-Griebenow, M. Zembala, and J. Pryjma. 2008. Peripheral blood CD14high CD16+ monocytes are main producers of IL-10. *Scand. J. Immunol.* 67: 152–159.
24. Berry, M. P., C. M. Graham, F. W. McNab, Z. Xu, S. A. Bloch, T. Oni, K. A. Wilkinson, R. Banchereau, J. Skinner, R. J. Wilkinson, et al. 2010. An interferon-inducible neutrophil-driven blood transcriptional signature in human tuberculosis. *Nature* 466: 973–977.
25. Novais, F. O., L. P. Carvalho, S. Passos, D. S. Roos, E. M. Carvalho, P. Scott, and D. P. Beiting. 2015. Genomic profiling of human *Leishmania* braziliensis lesions identifies transcriptional modules associated with cutaneous immunopathology. *J. Invest. Dermatol.* 135: 94–101.
26. Speake, C., S. Presnell, K. Domico, B. Zeitner, A. Bjork, D. Anderson, M. J. Mason, E. Whalen, O. Vargas, D. Popov, et al. 2015. An interactive web application for the dissemination of human systems immunology data. *J. Transl. Med.* 13: 196.
27. Teles, R. M., T. G. Graeber, S. R. Krutzik, D. Montoya, M. Schenk, D. J. Lee, E. Komisopoulou, K. Kelly-Scumpia, R. Chun, S. S. Iyer, et al. 2013. Type I interferon suppresses type II interferon-triggered human anti-mycobacterial responses. *Science* 339: 1448–1453.
28. Wang, P., H. Qi, S. Song, S. Li, N. Huang, W. Han, and D. Ma. 2015. ImmuCo: a database of gene co-expression in immune cells. *Nucleic Acids Res.* 43(D1): D1133–D1139.
29. Wang, P., Y. Yang, W. Han, and D. Ma. 2015. ImmuSort, a database on gene plasticity and electronic sorting for immune cells. [Published erratum appears in 2016 *Sci. Rep.* 6: 20996.] *Sci. Rep.* 5: 10370.
30. Potter, J. L., J. Narasimhan, L. Mende-Mueller, and A. L. Haas. 1999. Precursor processing of pro-ISG15/UCRP, an interferon-beta-induced ubiquitin-like protein. *J. Biol. Chem.* 274: 25061–25068.
31. Narasimhan, J., J. L. Potter, and A. L. Haas. 1996. Conjugation of the 15-kDa interferon-induced ubiquitin homolog is distinct from that of ubiquitin. *J. Biol. Chem.* 271: 324–330.
32. Knight, , E., Jr., D. Fahey, B. Cordova, M. Hillman, R. Kutny, N. Reich, and D. Blomstrom. 1988. A 15-kDa interferon-induced protein is derived by COOH-terminal processing of a 17-kDa precursor. *J. Biol. Chem.* 263: 4520–4522.
33. Recht, M., E. C. Borden, and E. Knight, Jr. 1991. A human 15-kDa IFN-induced protein induces the secretion of IFN-gamma. *J. Immunol.* 147: 2617–2623.
34. Wang, W., Y. Yin, L. Xu, J. Su, F. Huang, Y. Wang, P. P. C. Boor, K. Chen, W. Wang, W. Cao, et al. 2017. Unphosphorylated ISGF3 drives constitutive expression of interferon-stimulated genes to protect against viral infections. *Sci. Signal.* 10: eaah4248.
35. Tamassia, N., M. Zimmermann, M. Castellucci, R. Ostuni, K. Bruderek, B. Schilling, S. Brandau, F. Bazzoni, G. Natoli, and M. A. Cassatella. 2013. Cutting edge: an inactive chromatin configuration at the IL-10 locus in human neutrophils. *J. Immunol.* 190: 1921–1925.
36. Ma, W., W. Lim, K. Gee, S. Aucoin, D. Nandan, M. Kozlowski, F. Diaz-Mitoma, and A. Kumar. 2001. The p38 mitogen-activated kinase pathway regulates the human interleukin-10 promoter via the activation of Sp1 transcription factor in lipopolysaccharide-stimulated human macrophages. *J. Biol. Chem.* 276: 13664–13674.
37. Nair, S., P. A. Ramaswamy, S. Ghosh, D. C. Joshi, N. Pathak, I. Siddiqui, P. Sharma, S. E. Hasnain, S. C. Mande, and S. Mukhopadhyay. 2009. The PPE18 of *Mycobacterium tuberculosis* interacts with TLR2 and activates IL-10 induction in macrophage. *J. Immunol.* 183: 6269–6281.
38. Zhang, D., and D. E. Zhang. 2011. Interferon-stimulated gene 15 and the protein ISGylation system. *J. Interferon Cytokine Res.* 31: 119–130.
39. Kimmey, J. M., J. A. Campbell, L. A. Weiss, K. J. Monte, D. J. Lenschow, and C. L. Stallings. 2017. The impact of ISGylation during *Mycobacterium tuberculosis* infection in mice. *Microbes Infect.* 19: 249–258.
40. Guerra, S., A. Cáceres, K. P. Knobeloch, I. Horak, and M. Esteban. 2008. Vaccinia virus E3 protein prevents the antiviral action of ISG15. *PLoS Pathog.* 4: e1000096.
41. Lenschow, D. J. 2010. Antiviral properties of ISG15. *Viruses* 2: 2154–2168.
42. Lenschow, D. J., C. Lai, N. Frias-Staheli, N. V. Giannakopoulos, A. Lutz, T. Wolff, A. Osiak, B. Levine, R. E. Schmidt, A. García-Sastre, et al. 2007. IFN-stimulated gene 15 functions as a critical antiviral molecule against influenza, herpes, and Sindbis viruses. *Proc. Natl. Acad. Sci. USA* 104: 1371–1376.
43. Morales, D. J., K. Monte, L. Sun, J. J. Struckhoff, E. Agapov, M. J. Holtzman, T. S. Stappenbeck, and D. J. Lenschow. 2015. Novel mode of ISG15-mediated protection against influenza A virus and Sendai virus in mice. *J. Virol.* 89: 337–349.
44. Saraiva, M., and A. O'Garra. 2010. The regulation of IL-10 production by immune cells. *Nat. Rev. Immunol.* 10: 170–181.
45. Vivier, E., S. Ugolini, and J. A. Nunès. 2013. ADAPted secretion of cytokines in NK cells. *Nat. Immunol.* 14: 1108–1110.
46. Chan, S. H., M. Kobayashi, D. Santoli, B. Perussia, and G. Trinchieri. 1992. Mechanisms of IFN-gamma induction by natural killer cell stimulatory factor (NKSF/IL-12). Role of transcription and mRNA stability in the synergistic interaction between NKSF and IL-2. *J. Immunol.* 148: 92–98.
47. Chan, S. H., B. Perussia, J. W. Gupta, M. Kobayashi, M. Pospísil, H. A. Young, S. F. Wolf, D. Young, S. C. Clark, and G. Trinchieri. 1991. Induction of interferon gamma production by natural killer cell stimulatory factor: characterization of the responder cells and synergy with other inducers. *J. Exp. Med.* 173: 869–879.
48. D'Andrea, A., M. Aste-Amezaga, N. M. Valiante, X. Ma, M. Kubin, and G. Trinchieri. 1993. Interleukin 10 (IL-10) inhibits human lymphocyte interferon gamma-production by suppressing natural killer cell stimulatory factor/IL-12 synthesis in accessory cells. *J. Exp. Med.* 178: 1041–1048.
49. Hare, N. J., B. Chan, E. Chan, K. L. Kaufman, W. J. Britton, and B. M. Saunders. 2015. Microparticles released from *Mycobacterium tuberculosis*-infected human macrophages contain increased levels of the type I interferon inducible proteins including ISG15. *Proteomics* 15: 3020–3029.
50. Rider, P., E. Voronov, C. A. Dinarello, R. N. Apte, and I. Cohen. 2017. Alarmins: feel the stress. *J. Immunol.* 198: 1395–1402.